J. Phys. D: Appl. Phys. **32** (1999) 3013–3018. Printed in the UK PII: S0022-3727(99)03456-7

Exploratory studies on a passively triggered vacuum spark

R K Rout†, S K H Auluck†, J S Nagpal‡ and L V Kulkarni†

† High Pressure Physics Division, Bhabha Atomic Research Centre, Mumbai, India 400 085
‡ Radiation Standards and Instrumentation Division, Bhabha Atomic Research Centre, Mumbai, India 400 085

E-mail: rkrout@apsara.barc.ernet.in

Received 13 April 1999, in final form 14 September 1999

Abstract. The results of an experimental investigation on a passively triggered vacuum spark device are presented. The diagnostics include the current, x-ray and optical emission measurements. The sharp dips in the current derivative signal indicate the occurrence of pinching at an early stage of the discharge (at current ≈5 kA). A well-confined plasma with a central hot region was recorded using a streak camera. The pinched plasma was observed to undergo kink-type oscillations with a time period of 10–15 ns. Repeated plasma fronts were seen to move from the anode to the cathode with an average velocity of $\approx 5 \times 10^6$ cm s^{-1}. Soft x-ray emission having a radiation intensity of a few hundred mR per discharge was observed. The x-ray signals obtained using photodiodes showed multiple bursts. A soft x-ray pinhole camera recorded micro-pinches of ≈100 μm. The x-ray emitting regions were confined to the inter-electrode gap. The x-ray emission characteristics were influenced by the electrolytic resistance, which was connected across the spark gap to initiate discharge.

1. Introduction

Pulsed x-ray sources have wide applications in the field of microscopy, microlithography, flash radiography etc. As a pulsed x-ray source, the vacuum spark (VS) has been studied extensively (Lie and Elton 1971, Negus and Peacock 1979, Wong and Lee 1984, Chuaqui *et al* 1998). A VS is essentially a pulsed plasma, formed between two properly shaped electrodes by the discharge of electrical energy stored in a capacitor bank. We are mainly concerned with two types of VS; the untriggered (self-triggered) type and the triggered (by a pulsed laser or an auxiliary discharge) type. An untriggered VS requires a comparatively higher operating voltage, has a low x-ray emission yield and its reproducibility is very poor. A triggered VS needs an auxiliary power source or a high power pulsed laser synchronized with the VS discharge. Usually two distinct phases of x-ray emission are reported (Cohen *et al* 1968, Skowronek *et al* 1989). The first phase refers to the beam target x-rays emanating from the anode and the second phase is associated with pinching and subsequent breakup of the pinched plasma. One or more micro-pinches formed at the second stage are responsible for the emission of intense x-rays. Normally, the emission of x-rays in a VS plasma lasts for a few nanoseconds to a few tens of nanoseconds (Hebach *et al* 1993). Most of the published works are related to the spectroscopic studies of x-ray emission from micro-pinches. This paper deals with studies on the operational and emission characteristics of a triggered VS where the triggering is achieved passively by use of an electrolytic resistance across the spark gap. Observation of an oscillatory plasma and the plasma current measurements are reported for the first time. Unlike conventional VS, the present device produces a pinched plasma emitting intense x-rays, even at a low discharge current.

2. The vacuum spark set-up

A schematic view of the device is illustrated in figure 1. The anode is made of copper and has a conical tip of 45° half-apex angle with a tip diameter of ≈4 mm. The cathode is made of stainless steel and is also conical with a tip diameter of ≈0.2 mm. The separation between the tips of the anode and cathode is ≈9 mm. A silica tube (outer diameter 28 mm, wall thickness 1.5 mm) separates the anode from the base of the cathode. A specially designed vacuum sealed electrolytic ($CuSO_4$) resistance is connected across the anode and a third electrode (copper), which is insulated from the grounded cathode by a teflon sleeve (8 mm outer diameter, 2 mm thickness). The value of the resistance is altered by varying the concentration of electrolyte. The device is housed inside a stainless steel vacuum chamber of size $20 \times 20 \times 50$ cm^3. The chamber is mounted directly over a 4 inch diffstack vacuum pump module and is maintained at a pressure of $\approx 2 \times 10^{-5}$ mbar. A single capacitor (7.2 μF, 26 kV) with an integrally mounted sparkgap acts as the energy source. The maximum current (short circuit) delivered by the capacitor is 160 kA at a charging voltage of 26 kV with a quarter cycle of 1.6 μs and voltage reversal of 0.8.

When the spark gap is switched on, the charging voltage appears across the small gap (2 mm) over the surface

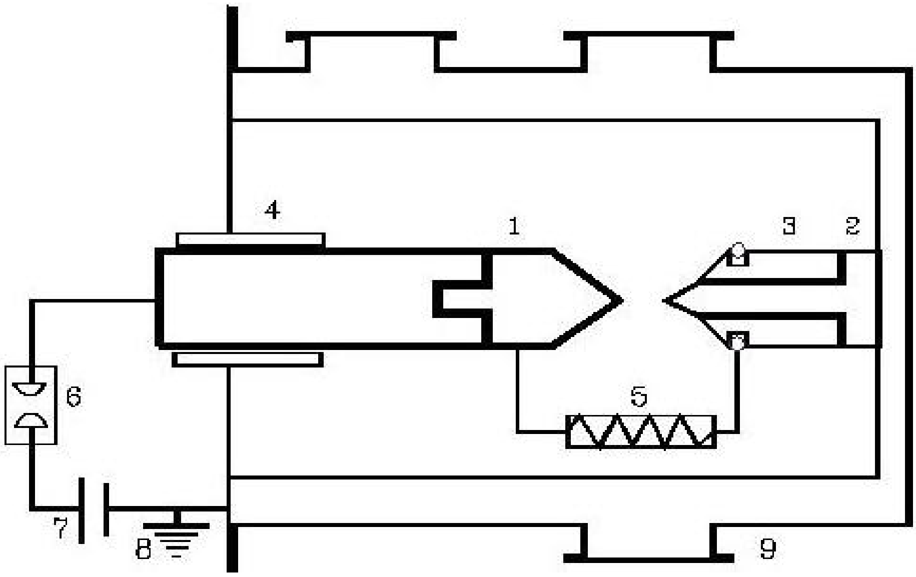

Figure 1. Schematic drawing of the vacuum spark set-up: 1, anode; 2, cathode; 3, teflon sleeve; 4, silica insulator; 5, electrolytic resistance; 6, spark gap; 7, capacitor; 8, ground; 9, vacuum chamber.

between the auxiliary electrode and the cathode via the electrolytic resistance. This leads to a sliding discharge on the teflon sleeve. Then the entire voltage appears across the electrolytic resistance, which gets connected to the cathode through sliding discharge plasma. The resistance prevents the collapse of the voltage across the anode–cathode gap until it is bridged by the plasma. The surface discharge helps in forming a pre-ionized plasma similar to a triggered vacuum spark. The electrons thus formed get accelerated within the gap towards the anode and evaporate the anode tip on bombardment. The anode plasma expands in the gap and begins the VS discharge. The nature (density and temperature) of pre-ionized plasma is governed by the current flowing through it, which in turn depends on the value of electrolytic resistance.

3. Current measurements

The rate of change of current ($\mathrm{d}I/\mathrm{d}t$) was measured using a miniature Rogowsky coil. One coil was mounted at the base of the anode and over the silica insulator to measure the current through the anode. The second coil was placed around the cathode, close to the VS gap, to monitor the plasma current. Vacuum sealed BNC connectors were used to bring the signals out of the chamber. The signals were routed through triaxial cables (RG58, 50 Ω). All the current signals were recorded using a 400 MHz Tektronix storage oscilloscope (TDS 744A) kept inside the Faraday cage. The signal integration facility of the oscilloscope was used to determine the current. All the Rogowsky coils were checked for the rise time and frequency response using a square-pulse signal, generated by charging a coaxial cable to 2 kV and discharging it into another terminated cable. The coils were calibrated *in situ* by discharge of the capacitor through the device at atmospheric pressure and using the damped sinusoidal current waveform as a standard.

The rate of change of current ($\mathrm{d}I/\mathrm{d}t$) through the anode and the plasma with respective integrated waveforms are

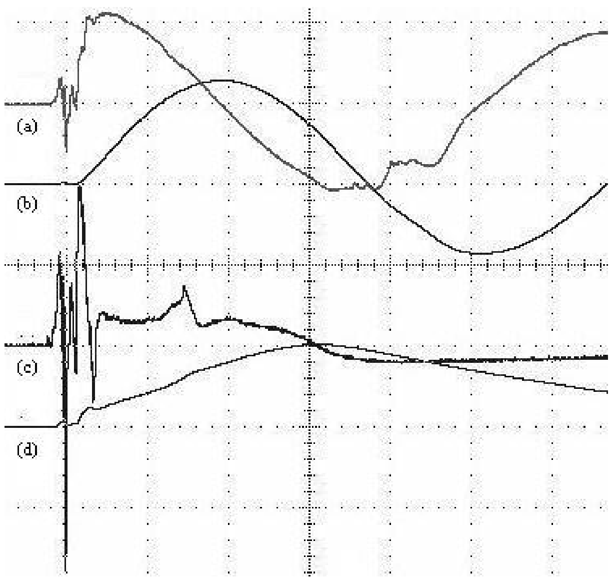

Figure 2. Current derivative and current signals from the vacuum spark: x-axis, 1 μs/division; y-axis, (*a*) anode $\mathrm{d}I/\mathrm{d}t$, $(1.1 \pm 0.1) \times 10^{11}$ A/s/division; (*b*) anode current, $(1.1 \pm 0.1) \times 10^{5}$ A/division; (*c*) plasma $\mathrm{d}I/\mathrm{d}t$, $(6 \pm 0.5) \times 10^{10}$ A/s/division; (*d*) plasma current, $(1.2 \pm 0.1) \times 10^{5}$ A/division.

shown in figure 2. Strong singularities indicating the collapse of the plasma were observed both in the plasma and the anode current derivatives. Multiple pinching seemed to occur in most of the discharges. In all the shots the first pinching occurred at an early stage of the discharge, when the plasma current was very low. The pinching was observed even at currents as low as 5 kA. The estimated energy coupled to the plasma at this instant is less than 2 J (assuming maximum inductance of the circuit). The plasma current (figure 2(*d*)) was observed to be always non-reversing in nature, whereas the anode/bank current (figure 2(*b*)) was damped sinusoidal.

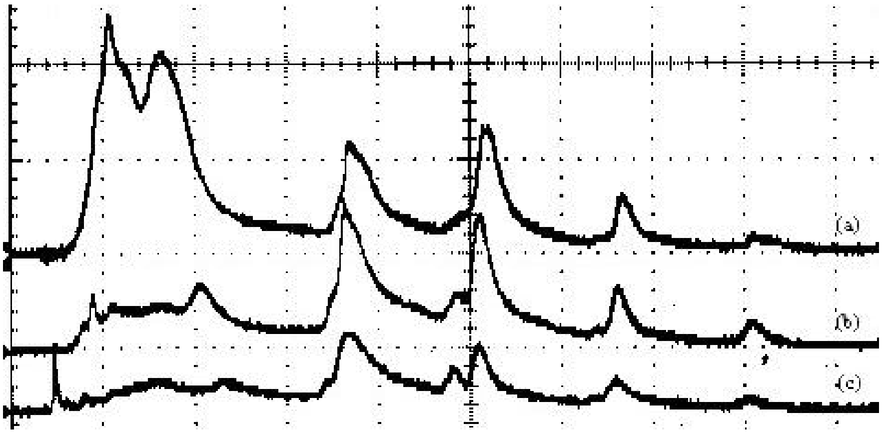

Figure 3. Optical signals through the photodiode: x-axis, 2 μs/division; y-axis, 0.5 V/division. (a) From cathode tip; (b) from middle point; (c) from anode tip.

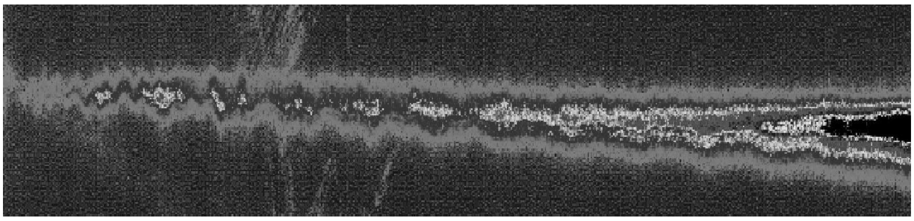

Figure 4. Streak image of the vacuum spark (10 ns mm^{-1} streak rate).

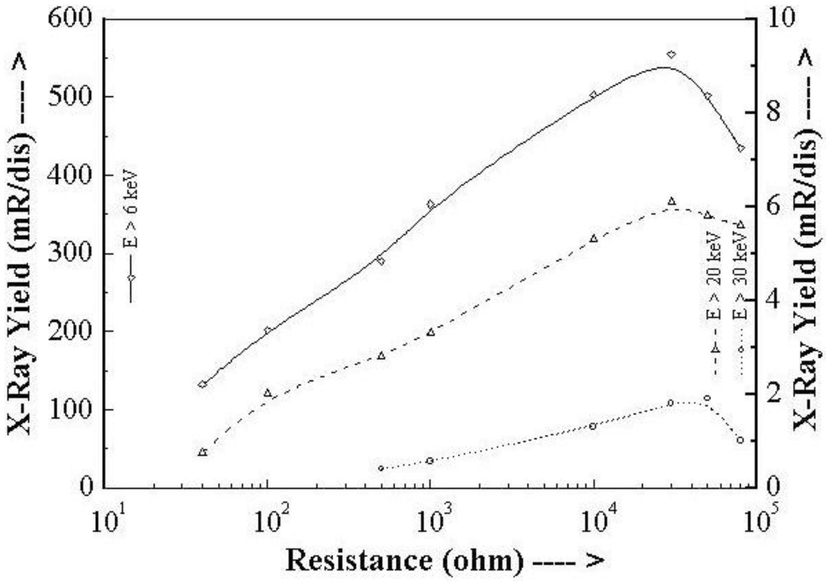

Figure 5. Average x-ray yield at different resistance values.

4. Optical emission study

Three regions (close to anode tip, middle point and close to cathode tip, <1 mm diameter each) within the VS region were focused with the help of a convex lens onto three separate optical fibres (1 mm diameter each) coupled to the photodiodes (FND-100, EG&G) and the temporal behaviours of the optical emission of these regions were recorded on a four-channel 100 MHz storage oscilloscope (GOULD 4074). The collecting area of the photodiode was 5 mm^2, the rise time and the fall time were <1 ns each. The optical signals (figure 3) indicate the occurrence of multiple plasma fronts moving from the anode to the cathode at a time much later than the current maximum. The average velocity of the fastest moving luminous plasma front was $\approx 5 \times 10^6$ cm s^{-1}. Assuming the plasma to be mostly copper ions, this velocity corresponds to an ion kinetic energy of $\approx$800 eV.

The light emission from a small region of the gap, 1 mm away from the tip of the anode was imaged through a streak camera (IMACON-790) with a slit (50 μm $\times$ 10 mm)

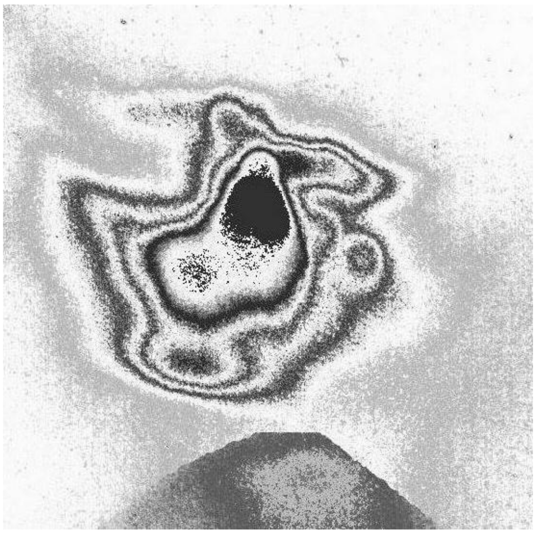

(*a*)

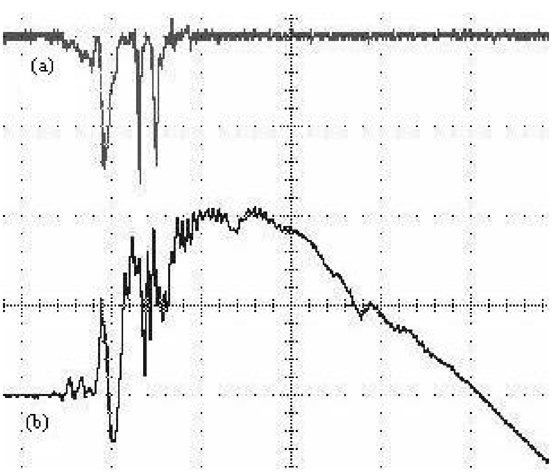

(*b*)

Figure 6. (*a*) x-ray pinhole image (50 Ω resistance, 400 μm pinhole, 4 μm Al–polycarbonate filter). (*b*) Signals corresponding to figure 6(*a*). x-axis, 0.5 μs/division; y-axis, (*a*) photodiode signal 2.5 V/division; (*b*) anode $\mathrm{d}I/\mathrm{d}t$ $(5.5 \pm 0.5) \times 10^{10}$ A/s/division).

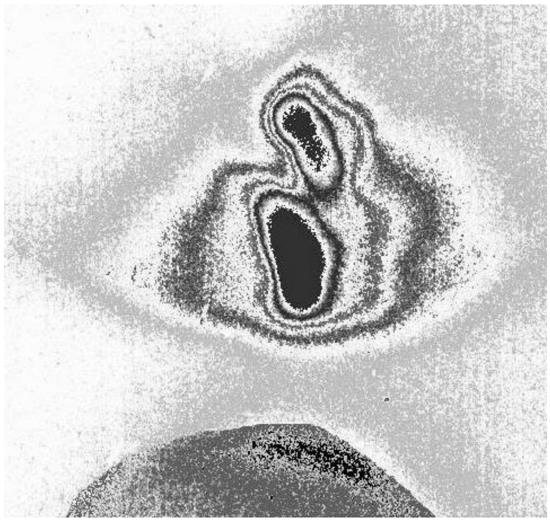

(*a*)

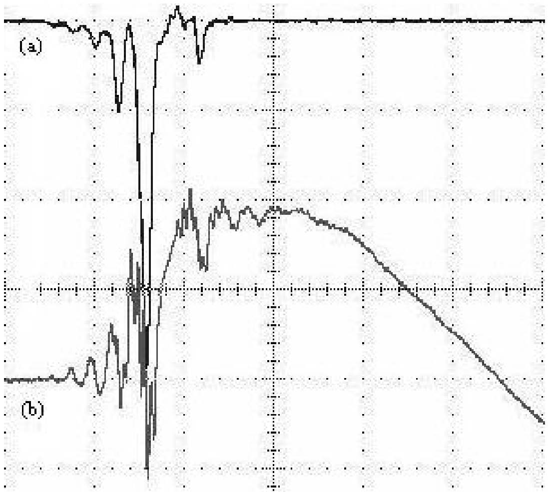

(*b*)

Figure 7. (*a*) x-ray pinhole image (2 kΩ resistance, 400 μm pinhole, 4 μm Al–polycarbonate filter). (*b*) Signals corresponding to figure 7(*a*). x-axis, 0.5 μs/division; y-axis, (*a*) photodiode signal 5 V/division; (*b*) anode $\mathrm{d}I/\mathrm{d}t$ $(5.5 \pm 0.5) \times 10^{10}$ A/s/division).

oriented perpendicular to the discharge axis. A typical streak photograph, at a streak rate of 10 ns mm^{-1}, is shown in figure 4. This shows a kink type oscillatory plasma with a dark central core embedded inside the luminous corona. The period of oscillation measured from the picture was 10–15 ns. The visible luminosity of free–free radiation at temperatures greater than a few eV varies as $n^2/T^{1/2}$, where n is density and T is the temperature of the plasma. Hence the dark central core within the luminous plasma can be interpreted as a hot pinch.

5. X-ray measurements

The x-ray yield of the VS was measured using teflon embedded-$CaSO_4$(Dy) thermoluminescent (TL) skived tape dosimeters. The dosimeters (8 mm diameter, 80 mg cm^{-2} thick) covered with various filters (0.09 mm Al, 2.3 mm Al, 0.23 mm Cu and 1.1 mm Cu) were positioned inside the vacuum chamber at a distance of 8 cm from the vacuum spark. Each time after eight discharges, the dosimeters were read for the integrated TL using a pre-calibrated TL reader (Nagpal *et al* 1995). The x-ray yield was estimated from the measured TL and its relative photon-energy response. The variation of average x-ray yield with the resistance (50 Ω–80 kΩ) is plotted in figure 5. For the x-ray energy $>$6 keV, the x-ray yield was 100–500 mR per discharge. It dropped down to 0.5–2 mR per discharge for energy $>$30 keV. Above energy 50 keV, the yield was below the threshold of measurement (0.02 mR/discharge). Maximum x-ray yield was observed in the case of $\approx$20 kΩ resistance. There was substantial generation of low-energy x-rays, close to the characteristic K x-rays (8 keV) of copper. Since only the anode tip (copper) was observed to be eroded, it was likely that the x-rays emanated mostly from the copper plasma. Production of higher energy x-rays might be assigned to the acceleration of the electrons and ions by the electric field generated by the

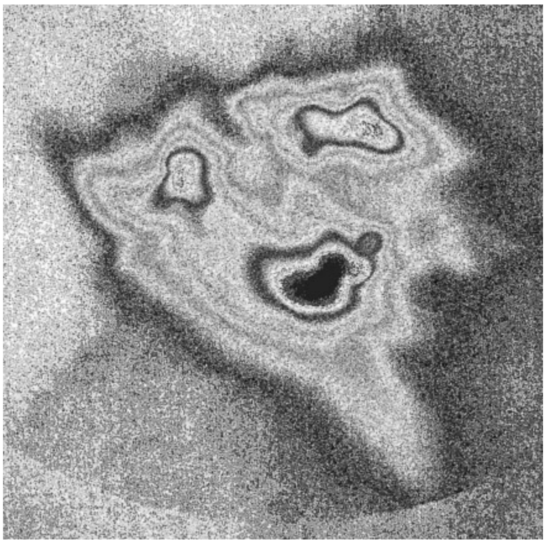

(*a*)

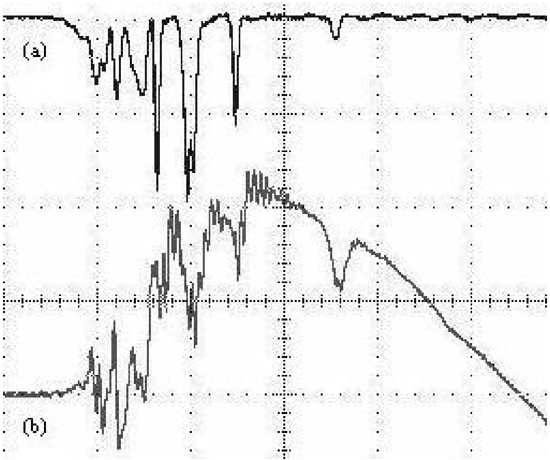

(*b*)

Figure 8. (*a*) x-ray pinhole image (50 k Ω resistance, 400 μm pinhole, 4 μm Al–polycarbonate filter). (*b*) Signals corresponding to figure 8(*a*). x-axis, 0.5 μs/division; y-axis, (*a*) photodiode signal 5 V/division; (*b*) Anode $\mathrm{d}I/\mathrm{d}t$ $(5.5 \pm 0.5) \times 10^{10}$ A/s/division).

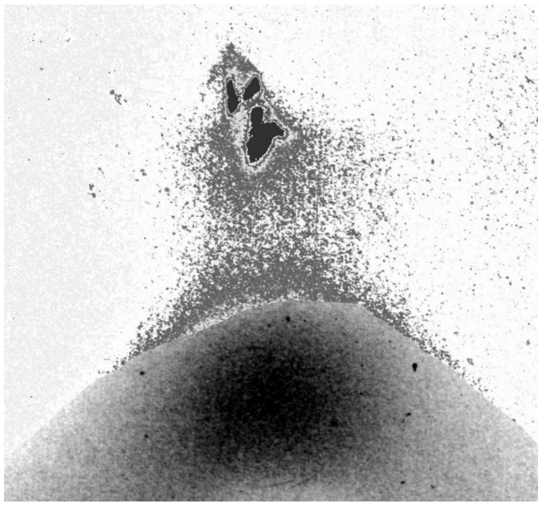

(*a*)

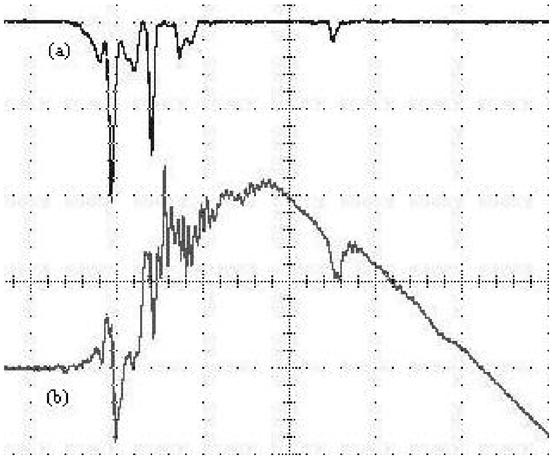

(*b*)

Figure 9. (*a*) x-ray pinhole image (2 k Ω resistance, 50 μm pinhole, 4 μm Al–polycarbonate filter). (*b*) Signals corresponding to figure 9(*a*). x-axis, 0.5 μs/division; y-axis, (*a*) photodiode signal 5 V/division; (*b*) Anode $\mathrm{d}I/\mathrm{d}t$ $(5.5 \times 0.5)10^{10}$ A/s/division).

applied voltage and the instabilities in the plasma (Fukai and Clothiaux 1975).

The temporal emission of x-rays was observed by soft x-ray sensitive silicon photodiode (windowless FND-100) covered with a thin (0.09 mm) aluminium filter. The diode output was recorded on a Tektronix 400 MHz storage oscilloscope. In general, multiple x-ray bursts were observed. One or two bursts were seen at an early stage of the discharge in most of the shots. A few bursts were seen at a later stage as well. The peaks of all the x-ray signals were approximately coincident with the corresponding sharp dips in the current derivatives. This suggested that the collapse/breakup of plasma could be the cause of the x-ray emission.

The time-integrated images obtained by a pinhole camera revealed the soft x-ray emitting structure of the VS plasma. A pinhole of 400 μm aperture, a 4 μm thick aluminized polycarbonate foil as filter and medical x-ray film (KODAK, X-Omat) were used in the camera. Up to six pictures could be recorded on a single film without breaking the vacuum. The pictures were scanned off-line by a 14-bit grey scale scanner in transmission mode. The image enhancement was achieved by an image processing technique which produced a contour-like pattern by de-emphasizing some intermediate gray levels. A few of the processed x-ray pinhole pictures obtained for different electrolytic resistances along with the corresponding photodiode and the rate of change of current signals are presented in figures 6–9. The lower structure in the figure is the anode tip. In figure 8(*a*) the anode tip masked by a hot plasma. The images clearly show that the x-ray emitting region is located within the VS gap and ≈2 mm away from the anode tip (except for shots with higher resistance). Most of the images indicated one or more micro-pinches (hot spots) embedded within the plasma. Generally, a diffused plasma with one or no hot spot was observed with lower values of resistance ($<$1 kΩ). Figure 6(*a*) is a pinhole picture of VS discharge with 50 Ω resistance. Figure 6(*b*) shows the corresponding x-ray photodiode and the current derivative signals. Similar results obtained with 2 kΩ and 50 kΩ resistances are shown respectively in figures 7 and 8. A well-confined plasma with a few hot spots was mostly seen in the images obtained with resistances of 1–20 kΩ. For a higher resistance (>40 kΩ) scattered hot spots showing the unstable nature of the plasma were observed as shown in figure 8(*a*). Figure 9(*a*) is an image obtained by using a smaller pinhole (50 μm diameter) and a 2 kΩ resistance. This image showed that the hot spots were of dimension $\approx$100 μm but non-symmetric. The probability of hot spot formation was less for the lower values of resistance and more for the higher resistance values. However, no quantitative correlation was found. At times, a straight plasma channel having multiple micro-pinches (dimension $\approx$100 μm) was also observed. The corresponding photodiode signal also indicated multiple bursts.

The first (initial) x-ray signal has generally been ascribed to the beam target interaction and subsequent signals to plasma pinching/breakup (Cohen *et al* 1968). However, in some shots in our experiment, especially at a low resistance value ($\approx$1 kΩ), a single early x-ray emission peak was seen with a single $\mathrm{d}I/\mathrm{d}t$ singularity. The corresponding x-ray pinhole picture showed a clear pinched plasma. This suggested that in our case, even the first x-ray pulse was caused by a collapsing hot plasma. The multiple x-ray bursts were accompanied by corresponding current singularities and zigzag x-ray pinhole pictures. These indicated that the plasma was subjected to repeated compressions at different times.

6. Conclusions

A simple way of generating VS plasma has been demonstrated using an electrolytic resistance across the VS gap. The energy spectrum of x-rays as well as the structure of the x-ray emitting zone are observed to be influenced by the resistance. The ionization (x-ray emission) seems to occur at a low current in this VS device. Therefore, this device can possibly be configured as an efficient spark ion source. The optical streak photograph suggests the oscillatory nature of the vacuum spark plasma. Leakage current of an unknown origin is speculated to be responsible for the non-reversing nature of the plasma current. This may be the general phenomenon in all the VS devices. However, to the best of our knowledge, direct measurement of the plasma $\mathrm{d}I/\mathrm{d}t$ as distinct from the total $\mathrm{d}I/\mathrm{d}t$ has not been reported so far. The intense x-ray emission has been recorded from a confined hot plasma even at a low current (<5 kA) and low energy (<2 J). The detailed mechanism involved in the formation of a concentrated plasma emitting intense x-rays even at a low current may be difficult to deduce with the data available at present. However, the pinching of plasma at a low current, deep current singularities and the observation of hot spots are likely to be the signature of electromagnetic collapse which is predicted (Meierovich 1984) to occur at currents less than 10 kA for a plasma where high-Z ions and significant axial heat conduction to electrodes are involved.

References

[1] Chuaqui H, Favre M, Saavedra R, Wyndham E S, Soto L, Choi P and Domitrescu-Zoita C 1998 *IEEE Trans. Plasma Sci.* **26** 1162–7

[2] Cohen L, Feldman U, Swartz M and Underwood J H 1968 *J. Opt. Soc. Am.* **58** 843–6

[3] Fukai J and Clothiaux E J 1975 *Phys. Rev. Lett.* **14** 863–6

[4] Hebach M, Schulz A, Kunze H J, Engel A and Lebert R 1993 *Europhys. Lett.* **21** 311–16

[5] Lie T N and Elton R C 1971 *Phys. Rev.* **3** 865–71

[6] Meierovich B E 1984 *Phys. Rep.* **104** 259–347 (see p 320)

[7] Nagpal J S, Udhayakyumar J, Page A G and Venkataraman G 1995 *Radiat. Protect. Dosimetry* **60** 181–4

[8] Negus C R and Peacock N J 1979 *J. Phys. D: Appl. Phys.* **12** 91–111

[9] Skowronek M, Romeas Paul and Choi Peter 1989 *IEEE Trans. Plasma Sci.* **17** 744–7

[10] Wong C S and Lee S 1984 *Rev. Sci. Instrum.* **55** 1125–8